Thermal Characterization of Rice Starches: A Polymeric Approach to Phase Transitions of Granular Starch

Costas G. Biliaderis,* Cheryl M. Page, Terry J. Maurice, and Bienvenido O. Juliano

The thermal properties of eight purified rice starches varying in physicochemical characteristics were investigated by differential scanning calorimetry (DSC) and thermomechanical analysis (TMA). There were significant correlations between DSC transition temperatures and gelatinization temperatures obtained by photometry, transition enthalpies and gelatinization temperatures, and volume expansion at 90 or 95 °C and amylose content. Although the Flory–Huggins theory for polymer melting fits the experimental data, it is not applicable to starch/water systems because of their irreversible (nonequilibrium) melting behavior. Water acts as a plasticizer (at <30% water content) of the amorphous parts of the granule and thus depresses their glass transition temperature (T_g). This induces crystallite melting to commence at lower temperatures. Both annealing and recrystallization take place during heating in the DSC, particularly at intermediate to low water contents. A three-phase model incorporating two distinct types of amorphous material and the crystalline domains of the amylopectin short-chain clusters is proposed to account for the thermal properties of granular starch/water mixtures. The TMA volume expansion curves of all nonwaxy (17–33% amylose) samples exhibited a two-stage swelling behavior. The first is associated with the onset of gelatinization phenomena (glass transition and partial melting) while the second coincides with the melting of starch crystallites.

INTRODUCTION

With the introduction of sensitive instrumentation in the last decade, thermal analysis techniques have rapidly gained prominence in food research. Recent reviews have highlighted the applications of thermal analysis in studying heat-related phenomena in foods and their constituents (Biliaderis, 1983; Lund, 1983; Wright, 1984).

The most common technique used in thermal studies of starches is differential scanning calorimetry (DSC). This technique, which detects the heat flow changes associated with both first-order (melting) and second-order (glass transition) transitions of polymeric materials, provided valuable insight into the order–disorder phenomena of granular starches (Donovan, 1979; Biliaderis et al., 1980; Donovan and Mapes, 1980; Kugimiya et al., 1980; Evans and Haisman, 1982; Burt and Russell, 1983). Thus, at intermediate water levels, two endothermic transitions were reported for the disorganization of starch crystallites, while a third endotherm at higher temperatures was attributed to the melting of amylose–lipid complexes. Furthermore, in view of the semicrystalline nature of the starch granule, attempts were made to treat starch gelatinization as a melting process (Lelievre, 1974; Donovan, 1979; Biliaderis et al., 1980; Evans and Haisman, 1982) by applying the Flory–Huggins equation (Flory, 1953). This expression relates the melting temperature of a semicrystalline polymer with the diluent concentration under equilibrium conditions. In recent studies, however, Maurice et al. (1985) and Slade and Levine (1984) have questioned the validity of this approach. They reported that starch gelatinization is nonequilibrium in character and that the process is controlled by the requirements for previous softening of the amorphous parts of the granule. The calorimetric data of Biliaderis et al. (1985) on isolated amylose–lipid complexes also led to similar conclusions. A process of partial melting followed by recrystallization and final melting during the DSC scan was proposed to account for their multiple-melting thermal profiles.

Because of the conflicting views on the mechanism of starch gelatinization, it was considered worthwhile to further investigate the effects of water on the phase transitions of granular starch, using eight purified rice starches of different physicochememical properties. In a previous DSC study of rice starches isolated from the same varieties, sodium dodecyl sulfonate (DoBS) was used to extract the protein (Russell and Juliano, 1983). However, this anionic detergent has been found to partially remove and replace the internal starch lipids (Maningat and Juliano, 1980). Therefore, the samples used in the present investigation were prepared from rice flours by using an alkaline protease (pronase) to remove protein. Pronase-treated starches gave the highest recovery in starch–lipid content with a minimum amount of residual contaminating protein (Maningat and Juliano, 1980). During the course of these studies, we found a sample of rice starch that showed the qualitative aspects of the thermal behavior of a two-phase semicrystalline polymer. This specimen thus provided an interesting opportunity to investigate the effects of water on the thermally activated processes of glass transition and crystallite melting. Furthermore, we have used thermal mechanical analysis (TMA, dilatometry mode) to monitor the volume expansion changes that accompany the phase transitions of these samples.

MATERIALS AND METHODS

The eight starch samples were prepared from milled rice flours using pronase (Calbiochem) according to Maningat and Juliano (1980). The methods used for the determination of the apparent amylose content, Kjeldahl nitrogen, lipids extracted by cold and hot water-saturated butanol (WSB), final birefringence end-point temperature (BEPT), and alkali viscogram gelatinization normality, have been previously described (Maningat and Juliano, 1979, 1980).

The DSC studies were carried out on a Du Pont 1090 thermal analyzer equipped with a pressure DSC cell. Details for the calibration and operation of this unit have been reported elsewhere (Maurice et al., 1985; Biliaderis et al., 1985). Pressure of 1400 kPa with N_2 was used to

Department of Food Science, University of Manitoba, Winnipeg, Manitoba, Canada R3T 2N2 (C.G.B.), Research Department, General Foods Inc., Cobourg, Ontario, Canada K9A 4L4 (C.M.P., T.J.M.), and Cereal Chemistry Department, International Rice Research Institute, Los Banos, Laguna, Philippines (B.O.J.).

0021-8561/86/1434-0006$01.50/0

Table I. Physicochemical and Thermomechanical (TMA) Properties of Rice Starches

sample	Kjeldahl N, %	amylose content, %	gelatinizn[a] temp, °C	WSB lipids, % cold	WSB lipids, % hot	alkali[b] gelatinizn, N	vol expnsn, % 90 °C	vol expnsn, % 95 °C	total area under TMA curve (arb units)
IR 29	0.02	2.1	67	0.20	0.24	0.36	64.1 ± 2.5[c]	108.7 ± 3.9[c]	86.2 ± 6.5[c]
RD 4	0.02	2.1	76	0.22	0.26	0.47	51.5 ± 4.6	103.1 ± 2.1	70.3 ± 5.0
IR 24	0.03	19.6	68	0.89	1.27	0.31	26.1 ± 0.7	39.3 ± 1.8	46.1 ± 0.4
IR 2071-137-5	0.03	17.4	77	0.78	1.10	0.48	22.3 ± 0.9	40.5 ± 0.8	36.3 ± 1.2
IR 480-5-9	0.08	28.7	60	0.94	1.65	0.27	20.6 ± 0.5	28.2 ± 1.8	48.6 ± 4.0
C4 63G	0.09	25.7	77	0.74	1.33	0.43	19.1 ± 2.6	28.0 ± 2.9	36.0 ± 8.4
IR 8	0.12	29.6	65	0.72	1.33	0.28	18.7 ± 1.5	20.7 ± 1.8	43.9 ± 6.5
IR 5	0.11	31.2	71	0.55	1.11	0.39	18.7 ± 0.4	22.6 ± 1.7	34.8 ± 1.5

[a] Photometric final gelatinization temperature. [b] Normality of KOH for 2.0% nonwaxy and 1.8% waxy to give 22.5 cp viscosity. [c] $n = 3$.

eliminate the problem of pan failure due to moisture loss at temperatures above 120 °C. Total sample weight was 7–12 mg. Ottawa sand was used as an inert reference material to balance the heat capacity of the sample pan. All starch–water samples of the desired moisture content were prepared in Du Pont coated aluminum pans and hermetically sealed. Characteristic temperatures of the transitions such as initial (T_i), peak (T_p), and completion (T_c) temperatures are shown in the thermal curves of Figure 1. The reproducibility of peak transition temperatures was generally ±0.3 °C. The volume fraction of water (v_1) in the samples was taken as the ratio of the total volume of water to that of starch plus water. The densities of water and starch were taken as 1.00 and 1.50, respectively. Theoretical treatment of the data according to the Flory–Huggins equation was carried out, using as T_m the T_c temperatures of the starch melting transitions and assuming that the Flory–Huggins polymer–diluent interaction parameter $X_1 = 0$. Under this assumption, the Flory–Huggins equation (eq 1) gives a linear relationship

$$1/T_m - 1/T_m^0 = \frac{RV_u}{\Delta H_u V_1}(v_1 - X_1 v_1^2) \qquad (1)$$

between v_1 and $1/T_m$, where R = gas constant, V_u/V_1 = ratio of molar volume of repeating unit to that of the diluent, T_m^0 = equilibrium melting point of undiluted polymer, T_m = melting point of polymer/diluent mixture, X_1 = Flory–Huggins polymer–diluent interaction parameter, v_1 = volume fraction of water, and ΔH_u = enthalpy of fusion per repeating unit. At low moisture levels, where the melting endotherms of starch crystallites and amylose–lipid complexes overlap, the T_c values were obtained either by extrapolation of the starch melting peak (if resolution permitted) or as the T_c temperature of the composite transition. After each DSC scan, the samples were cooled and rescanned.

A Du Pont 943 thermomechanical analyzer (TMA) equipped with a volume dilatometer probe was used to examine the volume expansion changes in 50% starch/water mixtures as a function of temperature (Maurice et al., 1985). Samples of 250 mg were firmly packed by using a 3.14-mm-diameter punch of a hand-operated puncture tester (Magness-Taylor type; applied force ca. 200g) into the dilatometer quartz vial. A thin layer of sand/paraffin oil mixture (5/1, w/w) was packed on top of the starch/water sample, and the vial was placed on the quartz stage of the TMA. The dilatometer (with zero weight load) was then lowered until it touched the surface of the sample and the instrument was zeroed. A heating rate of 2 °C/min was used for all experiments, and the temperature range was from 25 to 97 °C. Weight loss due to water evaporation during the TMA experiment was generally less than 7%, and it was taken into account for calculating the true volume expansion. All recorded linear dimensional changes were converted into volumes by the following equation (starch density 1.5):

$$\text{vol expnsn (\%)} = \frac{\text{(crs sectl area) (dimensnl chg (cor for } H_2O \text{ loss))}}{\text{init vol of starch}} \times 100$$

Data for both TMA and DSC were recorded at 0.4-s time intervals and stored on 8-in. floppy disks. Data analyses were performed by using the Du Pont software analysis programs. To facilitate comparisons between thermal curves, some of the data files were normalized to a constant sample weight.

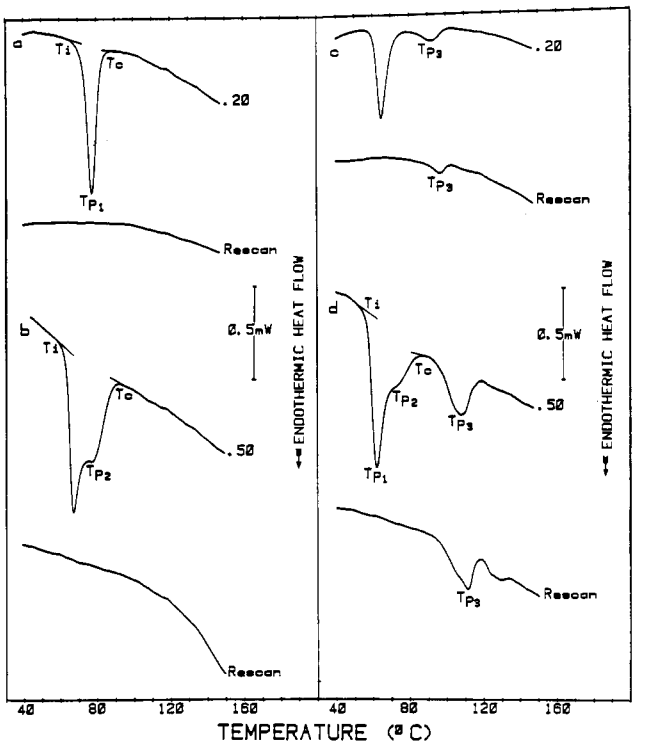

Figure 1. DSC thermal curves of rice starches at a heating rate of 10 °C/min. Numbers designate the weight fraction of starch. Sample identification and weight of solid material (mg): (a) RD 4, 2.06 (waxy); (b) IR 29, 4.77 (waxy); (c) IR 8, 1.88 (nonwaxy); (d) IR 480, 4.98 (nonwaxy).

RESULTS AND DISCUSSION

Differential Scanning Calorimetry (DSC). The physicochemical properties of the eight rice starch samples along with their thermal characteristics (DSC and TMA data) are presented in Tables I and II. Representative DSC thermal curves of waxy (2.1% amylose; a, b) and nonwaxy (17–33% amylose; c, d) starches at 80% and 50% water contents are shown in Figure 1.

Table II. DSC Characteristics of Rice Starches

sample	transitn temp, °C						transitn enthal, J/g	
	T_i	T_{P_1}	T_{P_2}	T_c	T_{P_3}	T_{P_3} rescan	starch	amylose–lipid complex
IR 29	60[a]	68.9		78			13.8 ± 0.6[c]	
	(60)[b]	(67.8)	(77)	(93)			(15.5)	
RD 4	65	77.6		86			17.1 ± 0.3	
	(63)	(77.0)	(87)	(100)			(18.7)	
IR 24	60	68.7		77	93, 114	99	11.8 ± 0.1	2.2 ± 0.2
	(61)	(68.9)	(79)	(92)	(109)	(112)	(13.2)	(2.2)
IR 2071-137-5	67	79.4		87	94	97, 114	15.3 ± 0.3	0.7 ± 0.3
	(68)	(81.6)	(88)	(98)	(108)	(112)	(16.4)	(1.7)
IR 480-5-9	54	61.5		70	91, 112	97, 114	8.6 ± 0.1	2.8 ± 0.1
	(53)	(61.9)	(74)	(87)	(108)	(111)	(11.5)	(3.2)
C4 63G	68	76.3		85	94	99, 111	13.6 ± 0.3	1.3 ± 0.1
	(67)	(75.8)	(86)	(97)	(109, 131)	(111, 132)	(15.2)	(2.5)
IR 8	56	64.9		77	92	97	10.2 ± 0.4	2.1 ± 0.2)
	(55)	(64.7)	(78)	(91)	(107)	(109, 126)	(11.7)	(2.7)
IR 5	66	73.1		82	94	99, 111	11.6 ± 0.3	1.4 ± 0.1
	(61)	(73.1)	(83)	(95)	(107)	(111, 126)	(13.3)	(1.8)

[a] Starch concentration 20%. [b] Numbers in parentheses are those of 50% starch concentration. [c] $n = 2$.

Table III. Simple Correlation Coefficients between Physicochemical Properties (Gelatinization Temperature, Amylose Content) and Thermal Characteristics (DSC, TMA)

	T_i[b]	T_{P_1}[b]	T_c[b]	ΔH		vol expnsn		total area under TMA curve
				starch	amylose–lipid[c]	90 °C	95 °C	
r_g[a]	0.95***	0.98***	0.98***	0.84**	−0.94***	ns	ns	ns
r_a[a]	ns[d]	ns	ns	ns	ns	−0.94***	−0.97***	−0.85**

[a] r_g, correlation with gelatinization temperature; r_a, correlation with amylose content. [b] Starch concentration of DSC experiment 20%. [c] Samples of waxy rice starch are not included. [d] Key: ns, nonsignificant; ***, $p < 0.001$; **, $p < 0.01$.

In addition to the endothermic peaks attributed to the disorganization of starch crystallites, all nonwaxy samples exhibited the reversible melting transition of the amylose–lipid complexes at temperatures above 95 °C (Figure 1). Differences in the DSC transition characteristics among the rice starches were also obvious. There was a good agreement between the DSC transition temperatures (T_i, T_{p_1}, T_c) and BEPT. These parameters were significantly correlated ($r = 0.95$–0.98; $p < 0.001$; Table III) as have been previously reported for cereal, legume, and tuber starches (Eberstein et al., 1980; Biliaderis et al., 1980; Russell and Juliano, 1983). The apparent gelatinization enthalpies for the rice starches ranged from 8.6 to 17.1 J/g (Table II; 20% starch). The correlation between ΔH and BEPT was significant ($r = 0.84$, $p < 0.01$) and accords with the findings of Russell and Juliano (1983); the more resistant the granule to gelatinization, the higher the energy required to disorganize its structure. It is also obvious from Table II that the nonwaxy samples had lower melting enthalpies than their waxy counterparts of similar BEPT. this observation can be explained by considering that crystallization (exothermic) of amylose–lipid complexes occurs simultaneously and immediately after the onset of the thermal events. This implies that the recorded DSC thermal profile represents the net thermal effect of two opposing processes: melting of starch crystallites and crystallization of amylose–lipid complexes. In rice starches, the internal granular lipids are mainly free fatty acids and lysophospholipids (lysolecithin) (Juliano, 1983). It is not clear, however, whether the monoacyl lipids exist as inclusion complexes with the linear starch component inside the granule or simply are tightly entrapped between the starch molecules and complex with amylose during heating (Morrison, 1981). Nevertheless, there is evidence that organization of amylose–lipid helices into supermolecular crystalline arrays does take place under starch gelatinization conditions. In fact, the apparent gelatinization enthalpy of defatted starch is greater than that of the native sample or defatted starch heated in the presence

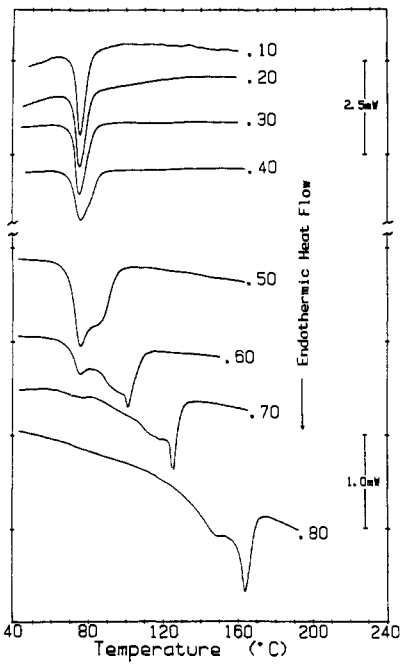

Figure 2. DSC thermal curves of RD 4 at various water contents. Numbers designate weight fraction of starch. Weight of starch from top to bottom (mg): 1.10, 1.96, 3.07, 4.02, 4.99, 5.27, 4.85, 4.57. Heating rate 10 °C/min. All data files were normalized to a constant sample weight of 5.00 mg.

of a monoglyceride (Page and Biliaderis, 1985). This indicates that complex formation followed by crystallization occurs exothermically during gelatinization. High BEPT nonwaxy samples exhibited lower melting enthalpies for the amylose-lipid complexes than their low-BEPT counterparts. This difference has been found to hold generally for both 20 and 50% starch/water mixtures (Table II).

The DSC thermal curves of a waxy (RD 4) and a nonwaxy (IR 8) rice starch heated in the presence of various amounts of water are shown in Figures 2 and 3 and 3

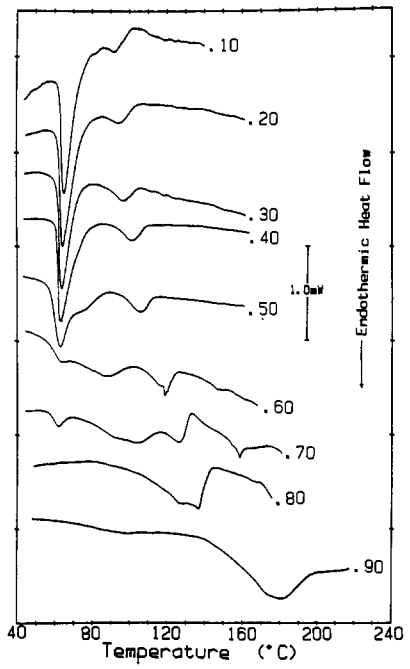

Figure 3. DSC thermal curves of IR 8 at various water contents. Numbers designate weight fraction of starch. Weight of starch from top to bottom (mg): 1.08, 2.03, 3.22, 4.03, 5.09, 5.41, 4.53, 5.61, and 3.96. Heating rate 10 °C/min. All data files were normalized to a constant sample weight of 5.00 mg.

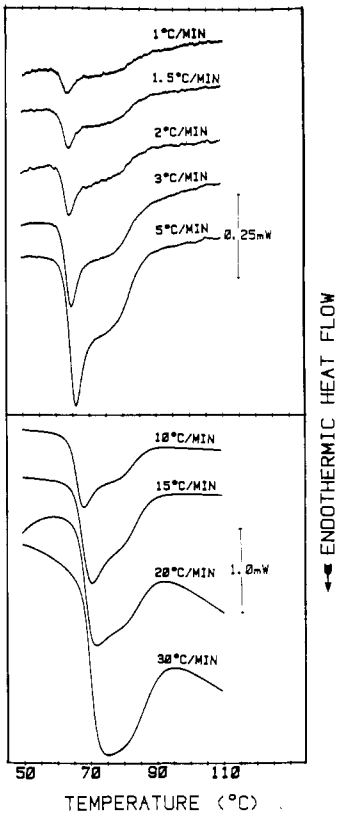

Figure 4. DSC thermal curves of IR 29 (50% w/w H_2O) at different heating rates. Weight of starch from top to bottom (mg): 4.99, 4.63, 4.65, 4.63, 4.65, 4.66, 4.66, 4.66, 4.68.

respectively. In starch/water mixtures containing more than 60% water, a single symmetrical endotherm was shown for the melting of starch crystallites. As the water content decreased, however, the size of this transition was progressively reduced with a concomitant development of a second, higher temperature, transition (P_2). These results are consistent with previous studies on other granular starches (Donovan, 1979; Biliaderis et al., 1980; Burt and Russell, 1983). It has been established that loss of birefringence is associated with the completion of the P_2 transition (Burt and Russell, 1983). Regarding the nature of these two endotherms, two models have been proposed. First, it was suggested (Donovan, 1979) that, upon hydration/swelling of the amorphous parts of the granule and due to their coupling with the crystallites, melting of the latter occurs cooperatively as long as water is present in the system in excess (first peak). However, when the amount of water becomes insufficient for this process to be completed, the remaining crystallites melt at higher temperatures (second peak); the T_{P_2} thus being dependent on the water content and the thermal stability of the remaining unmelted crystallites. This hypothesis focuses attention at the level of starch crystallite. An alternative explanation for starch gelatinization at intermediate water levels was given by Evans and Haisman (1982). They reported that the above biphasic endothermic transition reflects two types of melting. Granules that contain the least stable crystallites melt first cooperatively (P_1). Upon melting, the polysaccharide chains absorb more water and thus make it unavailable for the remaining ungelatinized granules. This means that the effective water concentration is further reduced by repartitioning of the water. Consequently, the ungelatinized granules will melt at even higher temperatures and thus give rise to the second transition (P_2). The attention here is shifted to the whole starch granule. Although both models were equivalent in that they postulated that melting is a solvent-facilitated process, they do not take into account that the starch granule, being a semicrystalline entity, can undergo reorganization during heating in the DSC. Marchant and Blanshard (1978), using a small-angle light-scattering device, have first suggested that, within partially gelatinized granules, there is possibility of rearrangements of the polymer chains in the amorphous phase and the remaining crystallites. There are also various lines of evidence that point out that reorganization does take place during the DSC scan. First, it is the variation seen in the thermal profiles as a function of the heating rate (Figure 4). At slow heating rates, immediately after the onset of the first peak and due to increased molecular mobility, there is greater opportunity for chain rearrangements in the crystallites. The so perturbed granular structure approaches a new equilibrium and thus a smaller fraction of crystallites will melt at low temperature (P_1). On the other hand, as the heating rate increases and because annealing is a relatively slow process, melting of more crystallites will occur during the first phase of the endothermic events. In fact, at the fastest heating rate used (30 °C/min), the melting profile did not show clear signs of the second endotherm; both transitions have merged into a single peak. Second, the sharp peaks seen in the low-moisture thermal curves at the concluding end of the endothermic profiles (e.g., Figure 2, 0.60, 0.70) provide additional evidence for melting of annealed/reorganized material. Third, aside from the fact that organization of amylose–lipid helices into a semicrystalline structure takes place during gelatinization, there is evidence that recrystallization of these materials occurs during the DSC scan. Two endothermic transitions have been assigned to the melting of these complexes at intermediate- or low-moisture levels without any reference, however, to their origin (Kugimiya et al., 1980; Wirakartakusumah, 1981; Bulpin et al., 1982; Donovan et al., 1983). On the basis of calorimetric findings on isolated amylose–lipid complexes, Biliaderis et al. (1985) have recently suggested that the multiple melting transition profile of these systems is a consequence of partial

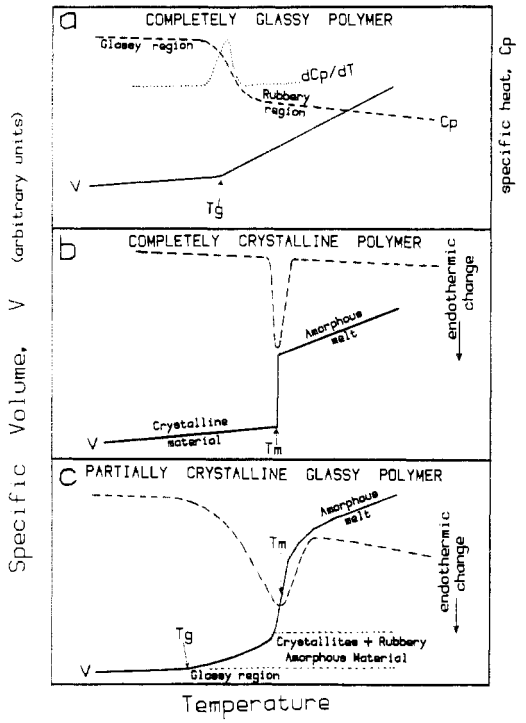

Figure 5. Generalized response of specific heat (dashed lines) and specific volume (solid line) vs. temperature for three idealized polymers in the glass transition and melting temperature regions (adapted from Jenkins (1972)).

melting followed by recrystallization and final melting. The exothermic effect often seen between the two endotherms (Figure 3, 0.70) provides supporting evidence that analogous reorganizational behavior of these complexes also occurs at the granular level. Furthermore, it demonstrates the nonequilibrium nature of the melting processes. Both annealing and recrystallization are greatly influenced by the water content; they become less prominent with increasing moisture level. Overall, the above discussion points out that the recorded thermal profiles of granular starches often represent the composite effect of various opposing processes that happen during the DSC heating experiment. Therefore, they are not indicative of the initial granular structure, particularly at intermediate- to low-water contents.

Starch Gelatinization from a Polymeric Perspective. The most important property of a polymer, affecting its physical properties, is the glass transition. The glass transition has many similarities to a second-order thermodynamic transition (Billingham and Jenkins, 1972). Thus, for a completely amorphous (glassy) polymer (Figure 5a) a gradual change is observed in the coefficient of thermal expansion which results in a change in slope of the specific volume vs. temperature curve at the glass transition temperature (T_g). This behavior parallels the changes in specific heat, as shown in Figure 5a, generating a maximum in the value of dC_p/dT (first derivative). A dramatic drop in modulus at T_g reflects the onset of segmental motion of the polymer chains. This is directly related to changes in the physical nature of the material that passes from a glassy to a rubberlike state. Analysis of this transitional behavior of a polymer by various methods is in fact based on the above T_g inherent property changes (Olabisi et al. 1979). On the other hand, phase changes occurring during melting of a crystalline structure are typical of a first-order process in which the thermodynamic functions show a sharp change (Figure 5b). Finally, in the case of a semicrystalline material, the situation is more complex. The specific heat or volume/temperature curve exhibits the characteristics of both glassy and crystalline polymers. The T_g and T_m determine the boundaries of the different phases as illustrated in Figure 5c. In a semicrystalline structure, many of the molecules are locked into crystallites. Furthermore, as the polymer chains are accommodated in the crystallites, the remaining nonordered segments are under tension and thus do not possess the typical characteristics of a bulk amorphous phase. Thus, changes in specific volume or heat at T_g become less conspicuous and more difficult to detect by dilatometry or other calorimetric methods. The above thermal behavior of a semicrystalline polymer becomes even more complicated in the presence of low molecular weight compounds (i.e., solvents and plasticizers in general) in the amorphous phase. Such compounds have been shown to depress both the glass transition (T_g) and the melting point (T_m) of a polymer. Water, for example, is a very effective plasticizer of natural and synthetic semicrystalline polymers (Marshall and Petrie, 1980; Bair, 1981; Jin et al. 1984; Maurice et al., 1985), causing a large depression in the T_g. The addition of small quantities of water to such materials produces an effect similar to an increase in temperature. This is so because the thermal and mechanical properties of the polymer are dependent on the difference between the testing temperature and the T_g. Furthermore, the depressing effect of a diluent on the T_m under equilibrium conditions can be expressed by using the Flory–Huggins approximation (Flory, 1953).

In view of the above thermal properties of semicrystalline polymers, we can now examine to what extent such principles can apply to phase transitions of starch. The starch granule is heterogeneous chemically and physically because it consists of amylose (linear) and amylopectin (branched) molecules as well as it has both crystalline and amorphous phases. Water in hydrated granules is primarily associated with the amorphous or gel phase (French, 1984) although it has been suggested that the crystal structure may also contain water of crystallization, particularly in the case of B-starch (Wu and Sarko, 1978). Crystallinity of the starch granules is generally in the order of 15–35%, as assessed by X-ray diffraction techniques (Banks and Greenwood, 1975). Consequently, the most simplistic model that can be used to describe morphologically such a semicrystalline structure would be a two phase system (fringed-micelle model) that assumes that the crystallites are dispersed in a homogeneous amorphous matrix and that the two phases behave independently of each other (Slade and Levine, 1984). In this case, one could expect to observe the thermally activated processes of glass transition and crystallite melting by DSC. Among the eight rice starches examined, distinct evidence for both first- and second-order transition phenomena was shown in the thermal curves of IR-2071 (Figure 6). An incremental change in heat capacity before the main melting peak was observed for the various starch/water mixtures examined. This heat capacity change is typical of an amorphous phase passing through the glass transition. In view of the plasticizing role of water (Maurice et al., 1985), we followed the manifestation of the thermal events in this sample over a wide range of moisture contents (0–90%). Figure 7 presents the dependence of T_g, T_p, and T_c (T_m) on the water content. All transition temperatures increase with decrease in moisture and converge to a high-temperature region at 240–250 °C for the dry sample. In particular, the T_g shows a monotonic increase at water contents lower than 30%. Above this level, T_g remains constant at 68 °C; i.e., activation (softening) of the

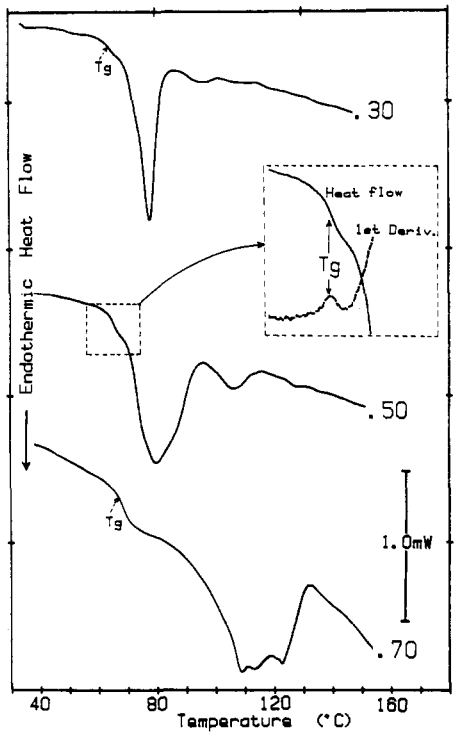

Figure 6. DSC thermal curves of IR 2071 at various water contents. Heating rate 10 °C/min. Numbers designate the weight fraction of the starch material. Weight of starch from top to bottom (mg): 3.06, 5.34, 7.54.

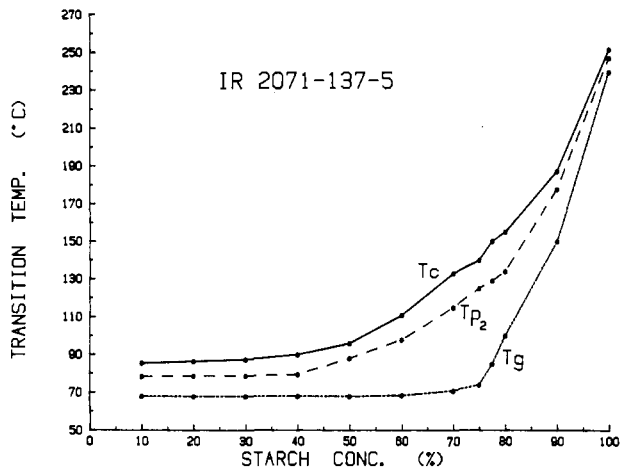

Figure 7. DSC characteristic transition temperatures (T_g, T_{P_2}, T_c) of IR 2071 as a function of starch concentration.

amorphous parts will take place only after exceeding this temperature. Therefore, the minimum requirement for water to fully exert its plasticizing effect on the granules of this sample is 30%. Interestingly, this value is within the range of water contents (28–33%) of underivatized granular starches in aqueous suspension of neutral pH (BeMiller and Pratt, 1981). This implies that, above this level, water forms a separate pure solvent phase outside the granules. The melting temperature of starch crystallites (T_c) is also depressed by water being, however, above the T_g under all conditions. The latter indicates that, regardless of the amount of water present, melting is T_g dependent in that a previous softening (relaxation) of the amorphous parts is required before crystallite melting can commence. This is also apparent from the Flory–Huggins plots of the melting data for RD 4 and IR-2071 (Figure 8). The experimental values showed a very good correlation between the volume fraction of water (v_1) and the melting temperatures (T_m) (r = 0.994, p <

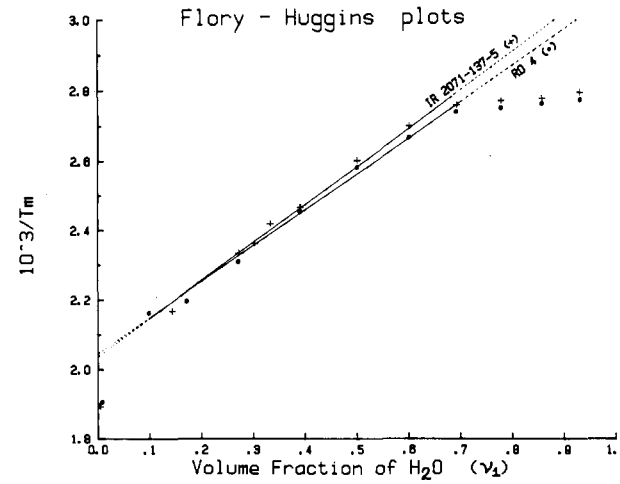

Figure 8. Flory–Huggins plots of melting data, $1/T_m$ (K) vs. volume fraction of water, for IR 2071 and RD 4. Each line is the linear least-square fit of the experimental data within the range 0.1–0.7 for the volume fraction of water (v_1).

0.001 for RD 4; r = 0.991, p <0.001 for IR 2071) at intermediate- or low-water contents (v_1 = 0.1–0.7). However, at v_1 < 0.7, a significant deviation between the experimental and the theoretical depression of T_m becomes evident. This is so because at high v_1 the depression of T_g upon plasticization of the granule by water remains constant and thus T_m cannot be further decreased at temperatures below the T_g. The theoretical prediction of T_m^0 by extrapolation to v_1 = 0 gave lower estimates than the actual experimental data for the dry samples; T_m^0 = 216 °C vs. 252 °C for RD 4, and T_m^0 = 218 C vs. 253 °C for IR 2071. Another complicating factor regarding the validity of using the Flory–Huggins equation (describes only equilibrium melting) is associated with the accuracy of detecting the true T_m values from the thermal curves. As it was stressed in the previous section, the DSC profile is not truly representative of the initial crystallite distribution, but it is a composite of melting and any reorganization that occurs during thermal analysis. Therefore, despite the good linear correlation in the data, there is indeed little theoretical basis in using this expression to follow the melting processes of starch/water systems.

Having established the nature of the transitions and the role of water, it is appropriate to further comment on the validity of the popular two-phase model as applied to starch as well as on the morphological/molecular origins of its DSC thermal profile.

The incremental change in heat capacity (ΔC_p) associated with the glass transition, as shown in the case of IR-2071 (Figure 6), is usually unobtainable with most of the granular starches. Thus, despite the relatively low degree of crystallinity of these materials, the melting peak appears as the main feature in their thermal profiles. For semicrystalline synthetic polymers, one finds that ΔC_p at T_g does not obey a simple quantitative two-phase relationship, but it is substantially reduced as the degree of crystallinity increases (O'Reilly et al., 1964; Jin et al., 1984). The crystalline regions act as physical cross links (Flory, 1974) that induce changes in the thermal properties of the amorphous material and thus suppress ΔC_p more than an ideal two-phase model would predict. Furthermore, there is evidence for a concomitant increase in the T_g (Buchanan and Walters, 1977; Jin et al., 1984). Studies on polycarbonate have shown that, at a degree of crystallinity as low as 23%, there is no detectable ΔCp at T_g (Wissler and Crist, 1980). To account for such behavior, the presence of two different types of noncrystalline material was sug-

gested: (a) bulk amorphous regions that are responsible for the ΔC_p at T_g; (b) intercrystalline material within spherulites that does not contribute to this heat capacity change. Given the clusterlike morphology of the amylopectin molecule (French, 1984), it would be interesting to consider the thermal behavior of granular starch by using the same insights. Amylopectin is the main crystalline entity in the granules of all waxy and low amylose content (<35%) starches (Robin et al., 1975; Banks and Greenwood, 1975; Biliaderis et al., 1981). Its semicrystalline character arises from the presence of (a) less organized regions of dense branching and (b) compact highly ordered areas (crystallites) of $\overline{DP}$ 15–20 chains. However, the overall organization of the molecule is such that it does not permit a sharp demarcation between the crsytalline and the amorphous regions since other longer chains ($\overline{DP}$ 50–60) run continuously from one phase to the other. Thus, the intercrystalline amorphous parts are under strain, and therefore it is likely that they do not have any of the thermal properties of an idealized amorphous phase (i.e., significant ΔC_p at T_g). On the other hand, there is no evidence that amylose participates in the crystallites of the above category of starches (Banks and Greenwood, 1975; French, 1984). This constituent can be considered as representing mainly the amorphous phase that is capable of activation at T_g. Accordingly, we propose that there are at least three factors influencing the incremental change in heat capacity and thus affecting the manifestation of second-order phemonena of granular starches. First, the ΔC_p at T_g is suppressed simply by chains being incorporated into the crystallites. The next factor is attributable to crystallinity induced physical cross linking that imposes restriction to segmental motion in the surrounding amorphous phase. Third, by analogy with synthetic semicrystalline polymers (Wissler and Crist, 1980; Jin et al., 1984) is the presence of the intercrystalline phase, which does not exhibit thermal behavior typical of a relaxed amorphous material. It is not surprising, therefore, that the T_g related ΔC_p is not usually observed in the thermal curves of starches. However, we feel that such thermally activated processes do take place at the leading edge of the first melting peak and thus are masked/superimposed by this transition. Furthermore, with reference to the original two-phase model, we also propose that the thermal behavior of granular starch can be best described by a three-phase model on the basis of its morphological and molecular features: a fully ordered crystalline phase, a bulk amorphous phase and a second nonordered intercrystalline phase. This model can also account for the multiple melting profiles observed at intermediate or low moisture contents. Thus, assuming the above complex morphology, there will be a concentration gradient for water between the fully crystalline and the bulk amorphous phase, where the majority of water resides in the latter. This implies that the plasticization behavior of the two amorphous phases will be dependent on the true plasticizer (water) content as well as on the nature of these regions. If this argument is valid, all T_g-controlled processes, melting and annealing of starch crystallites, and crystallization of amylose–lipid complexes would be affected differently at the various regions of the granular microstructure. With decreasing water content (i.e., T_m–T_g becomes wider), these thermally induced events will occur over a wider range of temperatures and thus yield broader and/or multiple transitions. Under such conditions, it is not surprising that the system usually assumes nonequilibrium (irreversible) melting during the course of the DSC heating experiment.

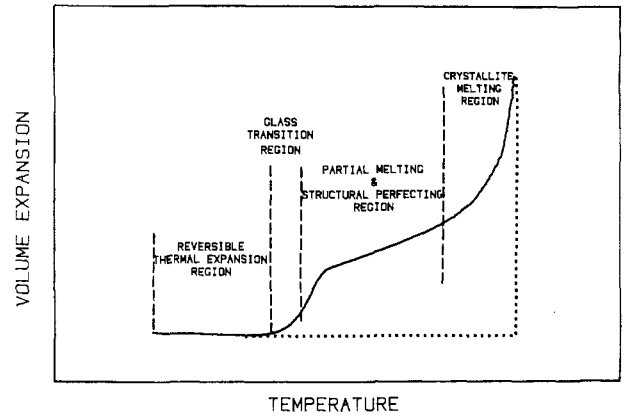

Figure 9. Typical TMA volume expansion curve of a nonwaxy rice starch. Dashed lines define the total area under the TMA curve.

Thermomechanical Analysis (TMA). A generalized swelling behavior, as revealed by a typical TMA curve, for a nonwaxy rice starch, is schematically illustrated in Figure 9. At least four different regions of volume expansion changes are noted: (1) From room temperature up to T_g, the sample undergoes reversible thermal expansion. (2) At T_g, the granules show an irreversible swelling due to the relaxation of the amorphous granular material (mainly amylose) not bound or loosely connected to crystallites. (3) The intermediate plateau region, above the T_g, where after partial melting the swollen granular structure does not show pronounced dimensional changes. Secondary phemonena such as annealing of starch crystallites and crystallization of amylose–lipid complexes may also occur in this region. (4) The abrupt volume expansion changes due to melting; tie molecules are pulling out of the crystallites as are the crystallites themselves from each other.

A useful presentation of DSC and TMA data for comparative purposes is that of Figure 10, where both the respective thermal curves are shown for each sample. It is interesting to note that, despite the different heating rates employed (10 °C/min for DSC vs. 2 °C/min for TMA), the onset of both endothermic and dilatometric events occurs in the same temperature region. This is indicative of the changes in specific heat and expansion coefficient when passing through the glass transition. Furthermore, the sharp volume changes seen at the conclusion of the TMA curves correspond with the melting endotherm of the starch crystallites. In all nonwaxy samples, the expansion behavior was strongly influenced by the presence of the linear starch component. One manifestation of this was the extended plateau in the TMA curves, following the glass transition region (Figure 10b, c). This effect can be attributed to the presence of (a) new crystallites involving bundles of amylose–lipid helices and/or (b) aggregated uncomplexed amylose chains or segments. These ordered domains are stable at temperatures below 100 °C; the former melt at 100–120 °C, while the latter at 140–160 °C (Biliaderis et al., 1985). Such structural elements can act as intercrystalline bridge-type cross links of large functionality to stabilize the polysaccharide gel network (Flory, 1974). As a result one would expect the volume expansion for the nonwaxy starches to be lower than that of the waxy samples. The corresponding values at 90 and 95 °C (Table I) as well as the significant correlation between volume expansion and amylose content (Table III) were indeed in accord with this concept. The absence of any distinct plateau region in the TMA curves of the waxy rice starches (Figure 10a), where the glass transition region is followed by first-order phe-

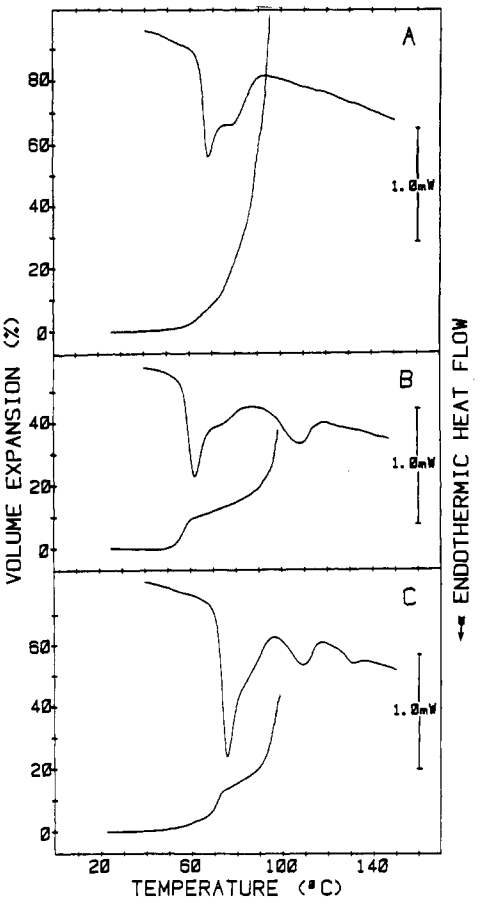

Figure 10. DSC and TMA thermal curves of three rice starches (50% w/w H_2O). Sample identification and weight (mg) of starch for DSC and TMA: (a) IR 29, 4.77, 127; (b) IR 480, 4.98, 123; (c) C4 63G, 5.36, 125. Heating rate for DSC 10 °C/min and for TMA 2 °C/min.

nomena, further substantiates the stabilizing role of the amylose molecules in the starch gel structure.

The calculated volume expansion values at 90 or 95 °C can be used for comparisons among various samples of different physicochemical properties. They may be also used as indices of rice quality since they are highly correlated ($r = -0.94$ or -0.97, $p < 0.001$; Table III) with the amylose content, the major determinant of eating quality of rice (Juliano et al., 1965; Juliano, 1979). Among varieties of similar amylose and lipid contents, differences in the gelatinization temperature can be assessed by the onset of the volume expansion curve (T_g region) or the total area under the TMA curve (Figure 9); the lower the BEPT, the lower the T_g and the greater the area under the curve (Table I). Therefore, the overall swelling profile may prove a good indicator of rice quality since it reflects the combined effect of amylose content, molecular properties of amylose and amylopectin, granular organization, and the presence of other nonstarch constituents (e.g., lipids).

CONCLUSIONS

The DSC and TMA studies of eight purified waxy (2.1% amylose) and nonwaxy (17–33% amylose) rice starches revealed differences in the thermal behavior of these materials. Thermal properties such as transition temperatures, enthalpies, and volume expansion characteristics were significantly correlated with other physicochemical properties (amylose content, BEPT, etc.) of the starch granules.

Evidence was provided that, at intermediate- to low-water contents, the DSC thermal curve is not representative of the initial crystallite profile. Instead, it reflects the composite thermal effect of several processes that occur simultaneously during heating in the DSC: melting, annealing, crystallization. This implies that melting of these systems is irreversible (nonequilibrium) and thus application of the Flory-Huggins equation (describes only equilibrium melting) to their melting data becomes problematic.

The order–disorder phase transitions of starch–water mixtures are analogous to those of semicrystalline synthetic polymers, whose thermomechanical properties can be drastically altered by the presence of small amounts of plasticizer molecules. Thus, the role of water (at levels <30%) is essential in that, acting as a plasticizer, it decreases the glass transition temperature of the amorphous parts of the granule. This in turn facilitates the melting or reorganization of the starch crystalites and amylose–lipid complexes to occur at lower temperatures. The DSC thermal profiles of an intermediate amylose content rice starch sample (IR-2071) provided evidence for both the thermally activated processes of glass transition and crystallite melting.

On the basis of the well-known morphological/molecular characteristics of the amylopectin molecule as well as the organization of the starch granule, a three-phase model is proposed to account for the thermal behavior of granular starch. Thus, it is suggested that, in addition to the starch crystallites, two distinct types of amorphous material exhibit different properties at T_g: first, a bulk amorphous phase (mainly amylose) that can undergo thermal activation at T_g (i.e., contributes to the incremental heat capacity change associated with second-order transitions); second, an intercrystalline amorphous phase (mainly intracrystalline regions of dense branching in the amylopectin molecules) that does not possess the typical properties that characterize the previous phase.

The TMA volume expansion curves (50% starch) of the nonwaxy samples exhibited a two-stage swelling pattern. The first is associated with the onset of the gelatinization phemonena (glass transition and partial melting), and the second, with the melting of starch crystallites. On the other hand, the waxy rice starches after the glass transition region mainly showed the second phase of volume expansion. This behavior clearly demonstrated the role of the linear starch fraction in stabilizing granule swelling during hydrothermal treatment.

Registry No. Starch, 9005-25-8; amylose, 9005-82-7; amylopectin, 9037-22-3.

LITERATURE CITED

Bair, H. E. In "Thermal Characterization of Polymeric Materials"; Turi, E. A., Ed.; Academic Press: New York, 1981; Chapter 9.

Banks, W.; Greenwood, C. T. "Starch and Its Components": Halsted Press: New York, 1975.

BeMiller, J. N.; Pratt, G. W. *Cereal Chem.* **1981**, *58*, 517.

Biliaderis, C. G.; Maurice, T. J.; Vose, J. R. *J. Food Sci.* **1980**, *45*, 1669.

Biliaderis, C. G.; Grant, D. R.; Vose, J. R. *Cereal Chem.* **1981**, *58*, 502.

Biliaderis, C. G. *Food Chem.* **1983**, *10*, 239.

Biliaderis, C. G.; Page, C. M.; Slade, L.; Sirett, R. R. *Carbohydr. Polym.* **1985**, *5*, 367.

Billingham, N. D.; Jenkins, A. D. In "Polymer Science"; Jenkins, A. D., Ed.; North-Holland Publishing Co.: Amsterdam, 1972; Chapter 2.

Buchanan, D. R.; Walters, J. P. *Textile Res. J.* **1977**, *47*, 398.

Bulpin, P. V.; Welsh, E. J.; Morris, E. R. *Staerke* **1982**, *34*, 335.

Burt, D. J.; Russell, P. L. *Staerke* **1983**, *35*, 354.

Donovan, J. W. *Biopolymers* **1979**, *18*, 263.

Donovan, J. W.; Mapes, C. J. *Staerke* **1980**, *32*, 190.

Donovan, J. W.; Lorenz, K.; Kulp, K. *Cereal Chem.* **1983**, *60*, 381.
Eberstein, V. K.; Hopcke, R.; Komieczny-Janda, G.; Stute, R. *Staerke* **1980**, *32*, 397.
Evans, I. D.; Haisman, D. R. *Staerke* **1982**, *34*, 224.
Flory, D. J. "Principles of Polymer Chemistry"; Cornell University Press: Ithaca, NY, 1953.
Flory, P. J. *Faraday Discuss. Chem. Soc.* **1974**, *57*, 7.
French, D. In "Starch Chemistry and Technology"; Whistler, R. L., BeMiller, J. N., Paschall, E. F., Eds.; Academic Press: New York, 1984; Chapter 7.
Jenkins, A. D. "Polymer Science"; North-Holland Publishing Co.: Amsterdam, 1972.
Jin, X.; Ellis, T. S.; Karasz, F. E. *J. Polymn. Sci., Polym. Phys. Ed.* **1984**, *22*, 1701.
Juliano, B. O.; Onate, L. U.; del Mundo, A. M. *Food Technol.* **1965**, *19*, 1006.
Juliano, B. O. In "Chemical Aspects of Rice Grain Quality"; International Rice Research Institute: Los Bãnos, Phillippines, 1979; p 69.
Juliano, B. O. In "Lipids in Cereal Technology"; Barnes, P. J., Ed.; Academic Press: New York, 1983; Chapter 15.
Kugimiya, M.; Donovan, J. W.; Wong, R. Y. *Staerke* **1980**, *32*, 265.
Lelievre, J. *J. Appl. Polym. Sci.* **1974**, *18*, 293.
Lund, D. B. In "Physical Properties of Foods"; Peleg, M., Bagley, E. B., Eds.; AVI: Westport, CT, 1983; Chapter 4.
Maningat, C. C.; Juliano, B. O. *Staerke* **1979**, *31*, 5.
Maningat, C. C.; Juliano, B. O. *Staerke* **1980**, *32*, 76.
Marchant, J. L.; Blanshard, J. M. V. *Staerke* **1978**, *30*, 257.
Marshall, A. S.; Petrie, S. E. *J. Photog. Sci.* **1980**, *28*, 128.
Maurice, T. J.; Slade, L.; Sirett, R. R.; Page, C. M. In "Influence of Water on Food Quality and Stability"; Simatos, D., Multon, S. L., Eds.; Nijhoff M. Publishers: Dordrecht, The Netherlands, 1985; p 211.
Morrison, W. R. *Staerke* **1981**, *33*, 408.
O'Reilly, J. M.; Karasz, F. E.; Bair, H. E. *J. Polymer Sci., Part C* **1964**, *6*, 109.
Olabisi, O.; Robeson, L. M.; Shaw, M. T. "Polymer-Polymer Miscibility"; Academic Press: New York, 1979.
Page, C. M.; Biliaderis, C. G. General Foods Inc., unpublished data, 1985.
Robin, J. P.; Mercier, C.; Duprat, F.; Charbonniere, R.; Guilbot, A. *Staerke* **1975**, *27*, 36.
Russell, P. L.; Juliano, B. O. *Staerke* **1983**, *35*, 382.
Slade, L.; Levine, H. In "Proceedings of the 13th North American Thermal Analysis Society Conference"; McGhie, A. R., Ed.; NATAS: University of Pennsylvania, Philadelphia, 1984.
Wirakartakusumah, M. A. Ph.D. Thesis, University of Wisconsin—Madison, WI, 1981.
Wissler, G. E.; Crist, B. J. R. *J. Polym. Sci. Polym. Phys. Ed.* **1980**, *18*, 1257.
Wright, D. J. *Crit. Rev. Appl. Chem.* **1984**, *5*, 1.
Wu, H. C. H.; Sarko, A. *Carbohydr. Res.* **1978**, *61*, 7.

Received for review May 13, 1985. Accepted September 9, 1985.

Effects of Seeding Time on Lipid Content and Fatty Acid Composition of Buckwheat Grains

Hirokadzu Taira,* Isamu Akimoto, and Takayoshi Miyahara

The effects of cropping season on lipid content and fatty acid composition of buckwheat grains were investigated on five cultivars by two seeding times. The early-seeding culture, as compared with the late-seeding culture, gave significantly higher lipid content and arachidic, behenic, oleic, and eicosenoic acid contents and lower linoleic and linolenic acid contents. The daily mean temperature during ripening showed significant positive correlations with lipid content and oleic acid content and negative correlations with linoleic and linolenic acid contents. As to the fatty acid composition, oleic and linoleic acids were main acids, and the dominant fatty acid was oleic acid in early-seeding culture and was linoleic acid in late-seeding culture. There was a highly negative correlation between oleic and linoleic acid contents.

Buckwheat grain is used as human food and also livestock and poultry feed. As for food, most of buckwheat is marketed in the form of flour. The flour is used primarily for making griddle cakes and is more commonly marketed in the form of pancake mixes than as pure buckwheat flour in U.S. (Marshall and Pomeranz, 1982). In Japan, however, buckwheat flour is mostly used for Soba, or Sobakiri (buckwheat noodle), which is prepared at Soba shops and at home from a mixture with 30–70% wheat flour. Japanese market for Soba making requires new crop seed because of the retention of greenish color of the testa and the fresh flavor of the grain. For Soba making, it is known that buckwheat flour must not be stored over 1 week after purchase because of the deterioration of its palatability. As one of the reasons for the deterioration during storage of the grain and after milling, it may be pointed out that lipid in the grain and flour is broken down by lipases into free fatty acids. The deterioration of buckwheat flour is faster than that of wheat flour because buckwheat flour contains embryo part, which is high in lipid content (Dorrell, 1971) and also lipase content. In the previous study on rice grain, it was shown that the temperature during ripening correlated with the lipid content and fatty acid composition (Taira et al., 1979). The seeding time of buckwheat is April to September in the south area and July to August in the north area in Japan. Accordingly, it was suggested that the seeding time or cropping season may affect lipid content and fatty acid composition of buckwheat grain. Little information is available on the influence of seeding time on lipid content and fatty acid composition of buckwheat grain. Therefore,

National Food Research Institute, Ministry of Agriculture, Forestry and Fisheries, Yatabe, Ibaraki 305, Japan (H.T.), and Tohoku National Agricultural Experiment Station, Ministry of Agriculture, Forestry and Fisheries, Morioka, Iwate 020-01, Japan (I.A., T.M.).

0021-8561/86/1434-0014$01.50/0